JOURNAL OF CATALYSIS 52, 157–168 (1978)

Selective Formation of Methanol from Synthesis Gas over Palladium Catalysts

M. L. POUTSMA, L. F. ELEK, P. A. IBARBIA, A. P. RISCH, AND J. A. RABO

Corporate Research Laboratory, Union Carbide Corporation, Tarrytown, New York 10591

Received June 24, 1977; revised November 10, 1977

Hydrogenation of carbon monoxide over supported Pd catalysts gave methanol in high selectivity at 260–350°C and 150–16,000 psig of pressure. Methanation became significant only outside the temperature–pressure regime for which methanol formation is thermodynamically favorable. The behavior of Pt and Ir appears similar although fewer data have been gathered. The catalytic behavior of these three noble metals toward synthesis gas is thus not only different from that commonly thought but also sharply contrasted with that of the other Group VIII metals for which ultimate C–O bond hydrogenolysis and hydrocarbon formation are a dominating feature. Silica-supported Pd was directly compared with Ni at 314°C and 12.25 atm of $CO:H_2$ (30:70); Pd not only gave methanol formation rather than the methanation observed for Ni but also much less chain growth activity than Ni. It is suggested that these differences in catalytic performance may be related to the inability of Pd (and Pt and Ir as well) to chemisorb CO dissociatively at reaction temperatures, compared to other Group VIII metals.

INTRODUCTION

The Group VIII metals all share the ability to hydrogenate carbon monoxide, largely with ultimate hydrogenolysis of the C–O bond and with varying extents of C–C bond formation. Nickel is the most thoroughly studied methanation catalyst (*1a*). Cobalt and iron are the classic Fischer–Tropsch catalysts for synthesis of higher hydrocarbons containing small amounts of terminally oxygenated products, especially alcohols (*2*). Chain growth to form polymethylene is maximized over ruthenium (*2*, *3*) at low-temperature–high-pressure conditions. Formation of C_2–C_4 terminally oxygenated products (carboxylic acids, aldehydes, and alcohols) is characteristic of rhodium at elevated pressures (*4*). In contrast, the catalytic properties of palladium, platinum, and iridium for synthesis gas conversion have been much less extensively described, although they have generally been considered to be relatively inactive catalysts and to form largely methane (*1*, *2b*, *c*, *4b*, *5*).

Vannice (*6*) recently compared the specific activities of all the Group VIII metals (except Os) for hydrogenation of CO at 1 atm of pressure (1 atm = 100.3 kN m^{-2}) in a differential reactor; chemisorption of CO was used to measure metal dispersion. The specific activity order at 275°C for metals supported on η-Al_2O_3 was: Ru > Fe > Ni > Co > Rh > Pd > Pt > Ir with a total range of ~100. In an early study by Fischer *et al.* (*7*) with unsupported metals of unknown dispersion, Pd ranked last in methanation activity. Under Vannice's (*6*) conditions, only hydrocarbon products were detected and the order of selectivity toward

0021-9517/78/0521-0157$02.00/0

methane formation was: Pd (no other significant product reported) > Pt > Ir > Ni > Rh > Co > Fe > Ru. This self-consistent data set (*6*) thus confirms the generalization made from earlier scattered data that Pd, Pt, and Ir are methanation catalysts of relatively low activity. The Pd catalysts were subject to sizable support effects (*8*): Pd/η-Al_2O_3 had some 80-fold the specific activity at 275°C of Pd black; even at identical dispersions, Pd/η-Al_2O_3 was some 45-fold more active than Pd/SiO_2; however, the high selectivity to methane was observed throughout. Under the quite different reaction conditions of ~500°C and 21 atm of $CO:H_2$ (1:3), Shultz *et al.* (*1*, *9*) reported a methanation selectivity of ≥98% for Pd and ~68% for Pt, the remaining products being higher hydrocarbons. Kertamus and Woolbert (*10*) reported a modest methanation activity for Pd/Al_2O_3 at 650°C and 1 atm. Eidus and co-workers (*11*) studied Pd/ThO_2/kieselguhr and Pt/kieselguhr catalysts at 250–300°C and 30–50 atm. Both were reported to have very low activity and to produce traces of methane. In a survey of noble metal catalysts at high pressure, Kratel (*12*) reported that Pd black at 280–400°C and 100 atm was comparatively inactive and gave traces of hydrocarbons but no oxygen-containing compounds.

We report herein that hydrogenation of CO over supported Pd catalysts produces methanol in high selectivity within the temperature–pressure regime for which methanol formation is a thermodynamically allowed process. The same behavior was found for Pt and Ir as well. This is then the first major exception to the observation that methanol formation from synthesis gas is typical of zinc oxide and its mixed oxides with Cr, Mn, and/or Cu (*13*), whereas hydrocarbon formation is typical of Group VIII metals. As we will show, there is no discrepancy between our observations and those of Vannice (*6*, *8*) or the Bureau of Mines group (*9*) because their temperature–pressure regimes were thermodynamically incompatible with formation of significant amounts of methanol. However, it is not clear why methanol was not observed by Eidus *et al.* (*11*) or Kratel (*12*).

EXPERIMENTAL

Catalyst preparations. A solution of 16.7 g of $PdCl_2$ in 200 ml of concentrated $HCl:H_2O$ (50:50, v/v) was absorbed into 200 g of silica gel (Davison Grade 57, 6 mesh) and excess liquid was removed in a rotary evaporator at 60°C *in vacuo*. The sample was then dried *in vacuo* at 150°C for 3 hr, activated in air at 300°C for 1 hr and

TABLE 1

Properties of Catalysts Employed

Designation	Metal	Support	Surface area ($m^2\ g^{-1}$)	Metal dispersion (%)	Metal crystallite size (Å)	Analysis (%)			
						Metal	Cl	C	H
A(B,C,L)	Pd	SiO_2	256	26	62	4.6	0.06	0.01	0.20
D	Pd	SiO_2	278	ND[a]	ND	0.50	0.03	ND	ND
E	Pd	γ-Al_2O_3	215	27	—[b]	4.8	2.9	0.03	0.59
G	Pt	SiO_2	249	25	254	5.0	0.04	ND	ND
H	Ir	SiO_2	219	44	27	4.3	0.38	ND	ND
M	Ni	SiO_2	ND	ND	158	2.7	ND	ND	ND

[a] Not determined.

[b] No Pd phase detected by X ray.

TABLE 2

Conversion of Synthesis Gas over Palladium Catalysts in a Tubular Flow Reactor

Run	Catalyst[a]	Temperature (°C)	Pressure (psig)	SV[b] (hr^{-1})	CO:H_2	Run time (hr)	Average rate of formation[c] (mol $liters^{-1}$ hr^{-1})		Final Pd crystallite size[d] (Å)
							CH_3OH	HCO_2CH_3	
1	A	275	16,000	3,300	30:70	4	5.8[e]	0.11	160
2	B	275	16,000	3,300	30:70	4	4.5	0.08	164
3	A	275	16,000	3,300	90:10	4	1.6	0.03	196
4	B	275	8,000	3,300	30:70	4	3.9	0.05	155
5	C	275	8,000	3,300	30:70	2	4.4	0.05	
6	C	275	8,000	3,300	30:65[f]	2	1.4	0.08	
7	B	325	8,000	3,300	30:70	4	15.2	0.27	202
8	B	325	4,000	3,300	30:70	4	9.7	0.12	129
9	B	350	1,500	3,300	30:70	4	7.1	0.03	—[g]
10	C	260	750	10,000	30:70	4	0.5	trace	
11	C	330	750	6,700	30:70	4	2.5	0.003	
12	C	325	150	3,300	30:70	4	0.48	trace	—[h]
13	D	275	8,000	3,300	30:70	2	0.13	trace	
14	E	275	16,000	3,300	30:70	4	3.3	0.18	489

[a] See Table 1.
[b] Feed volume at STP; bed volume = 30 ml, ~13 g for SiO_2-supported catalysts.
[c] For trace products, see text.
[d] From broadening of $2\theta = 40.15°$ X-ray line; initial size for A–C ~60 Å.
[e] Corresponds to 13.1% CO conversion.
[f] CO_2 in feed, 5%.
[g] Major line shows shoulders at lower 2θ values.
[h] Major line at ~39.1°.

at 400°C for 4 hr, cooled under argon, reduced in H_2 at 300°C for 2 hr and at 500°C for 2.5 hr, and finally evacuated and cooled. The analytical data, total surface area, Pd dispersion based on CO chemisorption with the assumption of 1:1 stoichiometry, and crystallite size determined from X-ray line broadening and the Scherrer equation are given in Table 1 for this catalyst, labeled A, and the other catalysts prepared. Catalysts B, C, and L were separate but operationally identical preparations with identical properties within experimental error. Catalyst D was prepared in the same manner except that one-tenth the amount of $PdCl_2$ was used. A solution of 33.4 g of $PdCl_2$ in 240 ml of concentrated HCl:H_2O (50:50, v/v) was absorbed into 400 g of γ-Al_2O_3 (Alcoa F-1, 6–8 mesh). Analogous drying and activation gave catalyst E.

TABLE 3

Conversion of Synthesis Gas over Noble Metal Catalysts in a Tubular Flow Reactor[a]

Catalyst	Metal	Average rate of formation (mol $liters^{-1}$ hr^{-1})	
		CH_3OH	HCO_2CH_3
—[b]	Pd	5.2	0.1
G	Pt	0.2	trace
H	Ir	0.33	0.007

[a] All runs for 4 hr at 275°C, 16,000 psig of CO:H_2 (30:70), and SV = 3300 hr^{-1}.
[b] Average of runs 1 and 2, Table 2.

A solution of 25 g of H_2PtCl_6 in 500 ml of water was evaporated in a rotary evaporator onto 200 g of silica gel *in vacuo* at 60°C. The sample was dried *in vacuo* at 150°C for 6 hr, activated in air at 300–400°C for 3 hr, reduced in H_2 at 300°C for 3 hr and at 500°C for 3 hr, and finally evacuated and cooled to give catalyst G. Catalyst H was prepared analogously from a solution of 13 g of $IrCl_4$ in 300 ml of water evaporated onto 100 g of silica gel.

A solution of 27.35 g of $Ni(NO_3)_2 \cdot 6H_2O$ in 250 ml of water was soaked into 200 g

TABLE 4

Conversion of Synthesis Gas over a Palladium Catalyst in a Gradientless Reactor[a]

SV (hr^{-1})	Exposure time (hr)	CH_3OH level in effluent[b,c] (mol %)	CH_3OH formation rate[b] (mol $liters^{-1}$ hr^{-1})
13,200	1.33	0.078	0.42
4,200	2.75	0.146	0.25
1,500	0.75	0.21	0.13
600	1.25	0.31	0.08
13,200	1.0	0.020	0.11

[a] Catalyst L (4.6% Pd/SiO_2) at 275–278°C and 11.9 atm of $CO:H_2$ (30:70).

[b] Measured at end of exposure period indicated for each SV.

[c] Lesser amounts of CH_4 detected but not quantified.

of silica gel; similar activation gave catalyst M.

Catalytic reactors. The data listed in Tables 2 and 3 were obtained with a high-pressure stainless steel tubular reactor ($\frac{7}{16}$ in. i.d. × 16″ long) containing a 30-cm^3 catalyst charge retained between plugs of stainless steel wool. Temperature was monitored and controlled by means of a coaxial thermocouple. The premixed feed gas (Linde) was passed through beds of activated coconut charcoal and Molecular Sieve 13X at cylinder pressure and then compressed into two 1-liter storage vessels to ~9000 psig, with a 10,000-psi stainless steel diaphragm-type compressor. The 16,000-psig pressure was obtained by pumping oil into the storage vessel with a Sprague 30,000-psi fluid pump. The catalyst was flushed with nitrogen, conditioned in flowing hydrogen at 275°C and 1500 psig overnight, depressurized and again flushed with nitrogen, and finally charged with the feed gas to the desired pressure from the storage vessels. Feed gas was then introduced at the desired constant rate by displacement from the storage vessel with

TABLE 5

Conversion of Synthesis Gas over an "Aged" Palladium Catalyst in a Gradientless Reactor[a]

Entry	Elapsed time (hr)	Temperature (°C)	Pressure (atm)	SV (hr^{-1})	CH_3OH level in effluent[b] (mol %)	CH_4: CH_3OH[b]	CH_3OH formation rate[b] (mol $liters^{-1}$ hr^{-1})
1	0[c]	290	12.25	2000	0.24	0.05	0.20
2	1	290	12.25	8000	0.064	0.06	0.21
3	3.5	290	12.25	800	0.37	0.07	0.12
4	5	290	12.25	2000	0.21	0.06	0.17
5	22.75	290	12.25	2000	0.23	—	0.19
6	25.5	290	3.1	800	~0.03	~0.6	~0.01
7	28[d]	290	28.2	800	0.98[e]	0.03	0.32[e]
8	28.5	290	28.2	800	1.13	0.05	0.37
9	32.5	290	12.25	2000	0.26	0.05	0.21
10	34.8	306	12.25	2000	0.22	0.08	0.18
11	51.5	314	12.25	2000	0.17	0.16	0.14
12	52.5	314	12.15	800	0.23	0.30	0.075
13	55.5	314	12.25	500	0.25	0.44	0.051

[a] Catalyst L (4.6% Pd/SiO_2) with $CO:H_2$ = 30:70.

[b] Measured at end of each period just before changing conditions for next entry.

[c] After 48.5 hr on stream; see text.

[d] A 68-hr period under N_2 at 290°C intervened between entries 6 and 7.

[e] Not all N_2 was removed; rate may be depressed; see entry 8.

pumped oil. Downstream from the reactor, pressure was reduced to 1500 psig by means of an Annin high pressure motor valve controlled by a remote, recording Foxboro controller, and the effluent gases were passed through a water-cooled scrubber containing ~100 ml of water to remove condensable products. The final pressure step-down from 1500 psig was performed with a Grove "Teflon" diaphragm back-pressure regulator. The off-gases were monitored by a wet-test meter and could be sampled on-line by gas chromatography. At the end of a run, the transfer lines were rinsed with water which was added to the scrubber. Used catalyst was soaked in water overnight; insignificant amounts of products were obtained although methanol could be detected.

The data in Tables 4 and 5 were obtained with a stainless steel Berty-type recirculating gradientless reactor (*14*) with 30 cm^3 of catalyst placed in the catalyst basket. The feed gas flow was controlled by a precalibrated Circle Seal fine-needle valve and a Grove "Teflon" diaphragm back-pressure regulator. All transfer lines were heated and led directly to a heated sampling valve after the back-pressure regulator for gas chromatographic analysis.

Analytical procedures. The aqueous product solution from the scrubber (always single phase) was analyzed by gas chromatography with use of a flame ionization detector and a silanized glass column (6 ft × 2 mm i.d.) of "Porapak N". By appropriate temperature programming between 100 and 160°C, the following oxygenated compounds could be routinely detected in synthetic mixtures: methanol, ethanol, *n*-propanol, isopropanol, *n*-butanol, isobutanol, acetaldehyde, propionaldehyde, *n*-butyraldehyde, acetic acid, propionic acid, *n*-butyric acid, acetone, and the formate and acetate esters of most of the alcohols. In all runs with Pd catalysts, the only detectable products with this column were methanol, methyl formate, and (at highest sensitivity) ethanol. Methanol and acetaldehyde were not resolved but were clearly separated on a column with β,β'-oxydipropionitrile liquid phase. The product assignment of methanol was confirmed by NMR spectroscopy. Quantitative data were obtained by peak integration and calibration based on an added acetone internal standard; occasional use of quantitative NMR confirmed the reliability of this procedure.

Traces of vicinal diols were determined at 120°C on a silanized glass column of "Carbowax 20M" polyethylene glycol on "Chromosorb T" with use of (nonlinear) calibration curves derived from standard solutions. Care must be taken to avoid "ghosting" by previous samples (*15*); preconditioning the column with H_2O was essential. Diol structures were confirmed by evaporating most of the methanol product and water from a scrubber aliquot, treating the residue with an excess of 1,1-dimethoxycyclopentane, and analyzing the resulting mixture by interfaced gas chromatography–mass spectroscopy. This reagent, after consuming residual water by ketal hydrolysis, converts diols to cyclic ketals the mass spectrum of which is dominated by a stable (M-29) ion presumably formed as shown below; the procedure was standardized with authentic diols.

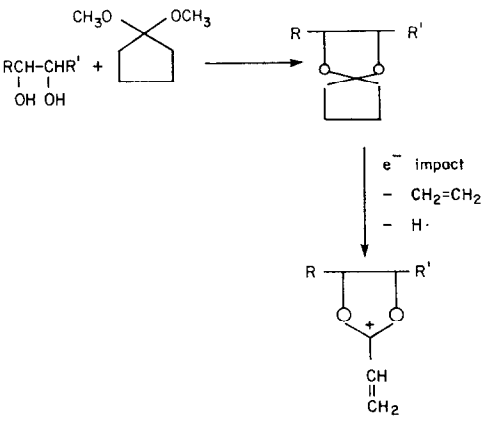

Gas analysis for CO, H_2, H_2O, CO_2, CH_4, C_2H_4, C_2H_6, O_2, and N_2 was performed by gas chromatography with use of a thermal conductivity detector and two columns (6 ft × 0.25 in. o.d. stainless steel) of "Porapak QS" and Molecular Sieve 5A connected in series through a four-way switching valve and operated at room temperature; sample injection was performed with a constant-volume gas sampling valve. In the first phase of the analysis with the columns in series, H_2 eluted from both columns (not quantifiable with He carrier gas); O_2, N_2, CO, and CH_4 passed through the "Porapak" column and proceeded onto the Molecular Sieve column; and the other components remained on the "Porapak" column. Value switching then connected the "Porapak" column directly to the detector to analyze for CO_2, H_2O, and the C_2 hydrocarbons while the Molecular Sieve column was dead-ended. Finally, returning the valve to the initial position allowed completion of the analysis of the components held on the Molecular Sieve column. For analysis of methanol and C_3 hydrocarbons when these were present in the gas phase, the same procedure was used except that the "Porapak" column was held at 80°C to hasten elution of these materials.

RESULTS

Performance of Palladium in a Tubular Reactor

Palladium catalysts supported on high-surface silica gel and γ-alumina were prepared by standard impregnation techniques. Catalysts were given arbitrary letter designations and are listed in Table 1. These were charged to a fixed-bed tubular flow reactor, conditioned overnight in flowing H_2 at 275°C and 1500 psig (1 psi = 6.8 kN m^{-2}), and then flushed with N_2 before beginning the CO–H_2 feed gas flow. Catalytic performance was evaluated in 2- or 4-hr runs as a function of temperature, pressure, space velocity [SV = (volume feed at STP)·(volume of catalyst bed)$^{-1}$·hours^{-1}], and CO:H_2 feed ratio. Condensable liquid products were scrubbed by cold H_2O at 1500 psig (or at reaction pressure, if lower) and analyzed at the conclusion of the run by gas chromatography and NMR spectroscopy; all liquid products were miscible with H_2O. The gaseous effluent was analyzed on-line by gas chromatography. Results are compiled in Table 2.

Methanol was the dominant product (typically 98–99% selectivity) over the range 260–350°C and 150–16,000 psig. The rates of methanol formation shown [moles·(volume of reactor bed)$^{-1}$·hours^{-1}] are averaged over the test period and therefore mask any effects of catalyst decay while on stream (see below). The only other easily detectable product was methyl formate, typically 1–2 mol% of the amount of methanol over Pd/SiO_2 catalysts. Occasional use of specific trace analysis techniques, however, revealed other oxygenated products at the level of <0.1 mol% of methanol. For example, runs 7, 8, and 9 gave ethanol at levels of 0.03, 0.04, and 0.14 mol% of methanol, respectively. All runs at ≥1500 psig gave minute amounts of vicinal diols. For example, run 2 gave ethylene glycol (0.05 mol% of methanol) and (tentatively assigned) propylene glycol, 1,2-butanediol, and 2,3-butanediols; the molar ratio of these diols was 1: ~0.7: <0.1: ~0.5. No methane nor any other gaseous hydrocarbons were found in superatmospheric runs at an analytical sensitivity which should have detected a methane formation rate of 0.015 mol liters^{-1} hr^{-1}. Thus for the highest methanol productivity encountered (at 325°C and 8000 psig of CO:H_2 = 30:70; run 7), the ratio CH_4:CH_3OH < 10^{-3}. In a run with catalyst C at 325°C and atmospheric pressure, traces of both methane and methanol were found.

Although the runs shown in Table 2 were not performed with the careful temperature control and low conversion levels required to derive accurate kinetic information, certain semiquantitative effects of reaction variables on the rate of methanol formation for the SiO_2-supported examples (runs 1–13) are readily apparent. Increased pressure at $CO:H_2 = 30:70$ and SV = 3300 hr^{-1} increased the rate at both 275°C (runs 1, 2, and 4) and 325°C (runs 7, 8, and 12). However, any attempt to determine the overall pressure exponent is futile because of the small spread in the data except for run 12 which, as we will show below, was equilibrium limited. The decreased rate with increased $CO:H_2$ ratio (runs 1, 2, and 3) shows that the pressure dependence on H_2 must be more positive than that on CO; this behavior is analogous to that for methanation at atmospheric pressure (*6*). Added carbon dioxide (runs 5 and 6) is mildly inhibitory. The temperature dependence, based on comparison of runs 4 and 7 at 8000 psig of $CO:H_2 = 30:70$ and of runs 10 and 11 at 750 psig, is relatively modest. Decreasing the Pd level on SiO_2 by a factor of 10 (runs 5 and 13 at 275°C and 8000 psig of $CO:H_2 = 30:70$) decreased the rate by an even greater factor of 34; this surprising phenomenon has not been investigated further. γ-Alumina support was comparably effective to SiO_2 (runs 1, 2, and 14); this behavior contrasts sharply with that reported (*8*) for methanation at atmospheric pressure for which η-Al_2O_3 was some 45-fold as effective as SiO_2 at comparable Pd dispersions and for which therefore a favorable electronic effect of the more acidic support was invoked.

Fresh Pd/SiO_2 catalysts had a metal dispersion of ~25% based on CO chemisorption and 1:1 surface stoichiometry [but see Ref. (*16a*)] and a metal crystallite size of ~60 Å based on X-ray line broadening. Examination of used catalysts after depressurization and removal from the reactor into ambient conditions revealed several changes from the fresh material. Chemical analysis showed no detectable Pd loss but some accumulation of carbon (~1.5% C for runs at 16,000 psig). Infrared spectra of degassed, used catalysts showed two sharp bands at ~2855 and ~2955 cm^{-1}. Since most of the carbon found by analysis as well as these C–H stretching bands could be removed by extraction with boiling H_2O, surface methoxylation of the SiO_2 support by the methanol product is implicated (*17*). For the runs at $\geq$4000 psig the Pd X-ray line at $2\theta = 40.15°$ narrowed, indicative of crystallite growth from ~60 to 150–200 Å. Used catalysts from lower pressure runs also showed an "extra" broadened line at lower 2θ values approaching that of the β-palladium hydride phase (*18*, *19*). This behavior may represent a residual β-PdH_x phase because of slow H_2 loss from slightly surface-contaminated samples (*20*) but was not studied further. Infrared spectra of adsorbed CO on fresh and used catalysts were compared by treating the samples in H_2 at 500°C, degassing, and exposing to 200 Torr (1 Torr = 133.3 Nm^{-2}) of CO at ambient temperature. Fresh catalysts showed the expected narrow band at 2085 cm^{-1} and a broad band at 1970 cm^{-1} (*21*). Used catalysts from runs 1 and 3 retained a significant amount of the lower frequency band but none of the >2000 cm^{-1} band. Such behavior has been associated (*22*) with the formation of more well-annealed Pd crystallites which expose a smaller fraction of high index planes. These data together thus indicate Pd mobility on the support under reaction conditions to give larger crystallites and loss of Pd surface area. The total surface area of the SiO_2-supported catalysts did not significantly change with use but that of catalyst E on γ-Al_2O_3 showed a decrease from 215 to 80 $m^2\ g^{-1}$ (run 14).

Performance of Platinum and Iridium

A comparison of Pd, Pt, and Ir, each supported on SiO_2, is shown in Table 3 for runs at 275°C and 16,000 psig of $CO:H_2$ (30:70). The latter two noble metals were at least an order of magnitude less active than Pd for comparable weight percentage loadings (approximately one-half the molar loadings) but they were fully analogous with respect to selective methanol formation.

Performance of Palladium in a Gradientless Reactor

The equilibrium constant for methanol formation can be calculated from standard thermochemical data (*23*) to be:

$$\log K_p \ (\text{atm}^{-2}) = \log\left[\frac{(P_{CH_3OH})(\gamma_{CH_3OH})}{(P_{CO})(\gamma_{CO})(P_{H_2})^2(\gamma_{H_2})^2}\right] = (5280)\cdot(1/T) - 12.78$$

which coincides reasonably well with the rather scattered experimental data available (*13b*). Assuming that the fugacity coefficient (γ) ratio will be near unity for relatively low pressures (*13b*), we can calculate approximate equilibrium-allowed conversions to methanol as a function of T (in degrees Kelvin) and

$$P = (P_{CH_3OH} + P_{CO} + P_{H_2}).$$

For example, at 325°C and 150 psig of $CO:H_2$ (30:70) (the lowest pressure entry in Table 2, run 12), the limiting calculated conversion is 0.7%; the actually observed conversion was 1.1%. Hence within the accuracy of the calculated K_p value and the ideality approximations involved, this run had achieved equilibrium. Of course, under these conditions the formation of methane is still highly allowed. Hence it was of interest to observe the $CH_4:CH_3OH$ ratio in the temperature–pressure regime where formation of the latter becomes seriously equilibrium limited. A second series of runs was therefore conducted in a back-mixed gradientless flow reactor of the type described by Berty (*14*) to achieve better temperature control and differential reactor conditions. Both methanol and methane were analyzed on-line as gases by use of a heated gas sampling valve and gas chromatography.

The initial observation under these conditions was a relatively rapid decay of activity with time on stream. An example is shown in Table 4 for Pd/SiO_2 at 275–278°C and 11.9 atm of $CO:H_2$ (30:70). The catalyst was conditioned overnight at 275°C and 150 psig of H_2; feed was then introduced and data were taken as a function of SV (effluent CO analysis confirmed that complete reactor flushing had occurred at the first sampling point). The instantaneous rate (proportional to the steady-state CH_3OH level in the well-stirred reactor) at a given flow rate appeared to decrease markedly with decreasing SV. However, return to the initial conditions after ~6 hr on stream revealed a fourfold decrease in rate. X-Ray line broadening indicated a parallel increase in Pd crystallite size from ~60 to ~200 Å, similar to that observed under much higher pressures in the flow reactor studies. Presumably a similar decay process in the early parts of the runs in Table 2 is concealed by the lack of instantaneous rate data.

More extensive data were collected from a run in which we first attempted to produce a "stabilized catalyst" after the initial rapid crystallite growth. Thus a catalyst was not only conditioned in H_2 as before but then was also exposed at 290°C to 12.25 atm of $CO:H_2$ (60:40) for 30.5 hr followed by $CO:H_2$ (30:70) for another 18 hr, all at SV = 2000 hr^{-1}. This procedure did indeed produce a relatively stable catalyst as shown in Table 5 by several comparisons of rate under identical conditions after

varying times on stream (for example, compare entries 1, 4, 5, and 9). In Table 5 the analytical data to determine instantaneous rate were taken for each entry at the elapsed time shown (plus the 48.5 hr of conditioning); the time allowed to achieve steady-state conditions at the conditions of any entry can be obtained by subtracting the elapsed time of the previous entry.

Changing the $CO:H_2$ feed ratio from 60:40 to 30:70 during the conditioning period led to a twofold rate increase (data not listed in Table 5), again indicative of a more positive pressure dependence on H_2 than CO. Entries 1–5 at 290°C and 12.25 atm probe the effect of SV; the calculated equilibrium level of CH_3OH is 0.85 mol%. The fourfold decrease from 8000 to 2000 hr^{-1} led to almost no change in rate, i.e., an almost fourfold increase in steady-state CH_3OH level from 0.064 (7.5% of equilibrium) to 0.23 mol% (27% of equilibrium). However, a further 2.5-fold decrease in SV gave a 1.6-fold decrease in rate as the CH_3OH level increased further to 0.37 mol% (44% of equilibrium). Such behavior would be expected either because of significant reversibility of CH_3OH formation or because of true product inhibition in the methanol-forming pathway. The precision of the data do not allow a decision. For this set, the ratio $CH_4:CH_3OH$ did not change significantly. Entries 11–13 form a second set of SV variation at 314°C and 12.25 atm. Here both a decline in CH_3OH formation rate and an increase in $CH_4:CH_3OH$ ratio occur. The CH_3OH level in entry 13 is 70% of equilibrium. Again the precision of the data does not allow us to decide whether the $CH_4:CH_3OH$ ratio finally begins to increase because of an independent route to CH_4 or hydrogenolysis of CH_3OH or both. Entries 3, 6, and 8 reveal the significant effect of increased pressure at constant temperature (290°C) and SV (800 hr^{-1}); flanking entries 1 and 9 indicate absence of catalyst aging over this period. Note again the sharp increase in $CH_4:CH_3OH$ ratio at the lowest pressure of 3.1 atm. Finally, entries 9–11 showed a small decrease in rate at 12.25 atm and SV = 2000 hr^{-1} when the temperature was increased by 24°C; this result is again most easily interpreted in terms of an increasing contribution from reversal of methanol formation.

Comparison with nickel. Nickel is generally recognized to give the most selective methanation and the least C–C bond formation of the common Fischer–Tropsch catalysts, i.e., Ni, Co, Fe, and Ru (*2*, *6*). To compare with Pd under identical conditions, a 2.7% Ni/SiO_2 catalyst (Table 1, catalyst M) was charged to the same gradientless reactor, flushed with N_2 overnight at 300°C and 12.25 atm, and then conditioned with $CO:H_2$ (30:70) for 3.75 hr at ~290°C, 12.25 atm, and SV ~12,000 hr^{-1}; there was evidence of rate decline during this period. Under stabilized conditions of 295°C, 12.25 atm of $CO:H_2$ (30:70), and SV = 14,000 hr^{-1}, the observed products were methane, ethylene, ethane, propylene, and propane in a molar ratio of 1:0.02:0.23:0.08:0.09 for a $C_1:C_2:C_3$ ratio of 1:0.5:0.5 on a carbon content basis. The total rate of CO consumption was 6.3 mol $liters^{-1}$ hr^{-1}. Even higher hydrocarbons may well have been formed since the analysis was truncated at C_3. *No* methanol could be detected. After 24 hr on stream, the CO consumption rate had decreased to 2.5 mol $liters^{-1}$ hr^{-1} but the molar ratio of the five hydrocarbons (1:0.03:0.26:0.09:0.06) had barely changed.

DISCUSSION

The hydrogenation of carbon monoxide over supported Pd catalysts is characterized by highly selective methanol production within the temperature–pressure regime for which the activity of the catalyst and the restraints of thermodynamics allow its formation. [The facile decomposition

of CH_3OH to CO and H_2 over Pd/asbestos has been reported (*24*) outside this regime.] Outside this range slower methanation occurs. The previous descriptions of selective methanation over Pd catalysts by Vannice (*6*) and Schulz and co-workers (*9*) were indeed for conditions outside the allowed methanol formation range. Thus at 275°C and 1 atm of $CO:H_2$ (1:2) feed (*6*), the equilibrium-limited, calculated final $CH_3OH:CO$ ratio is 3.2×10^{-4}; similarly at 499°C and 21 atm (*9*), $(CH_3OH:CO)_{eq}$ is 2.3×10^{-4}. In contrast, the studies by Eidus and co-workers (*11*) at 250–300°C and 30–50 atm were in the range where CH_3OH would have been expected but apparently was not observed. In their catalyst formulation (Pd/ThO_2/kieselguhr), thoria may well not be an inert component. The failure of Kratel (*12*) to observe CH_3OH at high pressures over Pd remains a puzzle; he did however report traces of CH_3OH over Pt catalysts.

At least at the very high pressures studied herein, Pt and Ir share the selectivity of Pd toward CH_3OH formation, albeit at lower rates.

Palladium thus stands in complete contrast with its congener Ni with respect to ability to cleave the C–O bond. It differs completely from its other nearest neighbor, Rh, in its comparative inability to catalyze C–C bond formation (*4*).

The mechanism of methanation over Ni has been widely studied (*1*) but is still the subject of active debate. Araki and Ponec (*25a*) recently described extensive static methanation studies on Ni films at 250–300°C and fractional Torr pressures from which they concluded that the initial step is dissociative chemisorption of CO followed by exhaustive hydrogenation of the resulting separate C and O adatoms. In this mechanism (*25*) complete C–O bond rupture precedes any hydrogenation and no partially hydrogenated, oxygenated intermediates (*1b*), which could be potential precursors of formaldehyde or methanol, are involved. Wentrcek and co-workers (*26*) carried out pulsed experiments and reached the same mechanistic conclusion. In this work it was demonstrated that a pulse of pure CO was disproportionated to gaseous CO_2 and surface carbon at >175°C and that the latter could subsequently be removed as CH_4 by a pulse of H_2. Similar studied by Rabo and co-workers (*27*) support this behavior for Ni/SiO_2 at 300°C. In contrast, parallel studies (*27*) with Pd/SiO_2 showed that pulsing with CO at 300°C gave only traces of CO_2. However, CO was retained, presumably in undissociated chemisorbed form, and could be largely methanated by subsequent pulses of H_2. (The H_2 pressure in pulsed experiments is too low to allow significant CH_3OH formation.) These pulsed studies thus show a sharp contrast in the abilities of Pd and Ni to adsorb CO dissociatively. Combining this information with the catalytic behavior reported herein, we suggest that the ability of Pd (and of Pt and Ir as well) compared with Ni to catalyze methanol formation to the virtual exclusion of methane under elevated pressure results from its excellent hydrogenation ability coupled with its inherent tendency to adsorb CO nondissociatively even at reaction temperatures.

The adsorption behavior of CO on transition metals at room temperature under UHV conditions has recently been summarized (*28*). Adsorption is nondissociative not only on Pd (*16*), Ir, and Pt, but also on Ni and Ru; only Fe gives evidence for CO cleavage. However, at >200°C, dissociation occurs also on Ni (*29*). Rhodin (*29a*) determined the energy separation between the 1π and 4σ levels of molecularly adsorbed CO by photoemission spectroscopy using synchrotron irradiation and suggested that increased level separation ($Pt < Ir < Pd < Ni \lesssim Ru < Fe$) was diagnostic of greater C–O bond lengthening

in the adsorbed state and therefore of a lowered activation energy for dissociation. [A resolution of the higher energy PES band of Pd into 1π and 5σ levels has been described (*30*)]. By this spectroscopic criterion, the tendency toward dissociation should be least for Pt and should increase as one proceeds upward and toward the left in the Periodic Table, in agreement with available chemisorption data. The order of heats of adsorption of O and C atoms, another factor which will contribute to the tendency toward dissociative chemisorption, also increases in a similar order throughout Group VIII (*28b*, *31*). We suggest then that the catalytically significant break at ~300°C with respect to retention of the C–O bond occurs between the lower right-hand triad, Pt, Pd, and Ir, and the rest of Group VIII.

The implication is thus that the mechanism of CH_3OH formation on Pd involves addition of adsorbed H atoms to adsorbed CO and must therefore proceed through partially hydrogenated CH_xO surface complexes. It is of interest to note that coadsorption of CO and H_2 at room temperature and UHV conditions on a Pd(110) surface leads to an ordered mixed surface structure as judged by LEED results but one with minimal interaction as judged by thermal desorption and work function studies (*32*). The rate response to $CO:H_2$ ratio suggests that H_2 competes poorly with CO for surface sites, in accord with known heats of adsorption (*6*, *32*).

Our data include cases (entries 6, 12, and 13 of Table 5) where the $CH_4:CH_3OH$ ratio increased when the formation of CH_3OH became equilibrium limited. However, we do not have sufficient data on product formation profiles vs time to indicate whether methane formation under these conditions occurs by hydrogenolysis of methanol as an intermediate or by an independent pathway from CO and H_2 parallel to that of methanol formation.

It has been demonstrated for certain reactions involving H_2 that the α-Pd-H solid solution and β-Pd–H phase can possess differing catalytic activities (*18*, *33*). Most of our experiments were carried out at temperatures and pressures high enough so that these phases merged (*18*, *19*). However, some of those in Table 5, chosen to represent temperature–pressure conditions restricting CH_3OH formation, thereby fall near the critical solution temperature and pressure (300–310°C and 20 atm H_2) for the bulk α and β phases. Hence there is an ambiguity in specifying the composition of the metal phase(s) at this point, particularly if small particles are dominated by surface effects which lead to deviations from bulk phase diagrams (*33*). Whether this has any secondary relationship to our catalytic results is not apparent.

ACKNOWLEDGMENTS

The authors wish to acknowledge C. L. Angell for determining the infrared spectra of catalysts and I. R. Ladd for carrying out the interfaced gas chromatographic–mass spectral analysis for diols. Determination of metal dispersions was performed by F. G. Young.

REFERENCES

1. (*a*) Mills, G. A., and Steffgen, F. W., *Catal. Rev.* **8**, 159 (1973); (*b*) Vannice, M. A., *Catal. Rev. Sci. Eng.* **14**, 153 (1976).
2. (*a*) Storch, H. H., Golumbic, N., and Anderson, R. B., "The Fischer–Tropsch and Related Syntheses." Wiley, New York, 1951; (*b*) Pichler, H., *Advan. Catal.* **4**, 271 (1952); (*c*) Anderson, R. B., *in* "Catalysis" (P. H. Emmett, Ed.), Vol. 4. Reinhold, New York, 1956; (*d*) Pichler, H., and Hector, A., "Kirk–Othmer Encyclopedia of Chemical Technology," 2nd ed., Vol. 4, p. 446. Wiley, New York, 1964; (*e*) Pichler, H., and Schulz, H., *Chem. Ing. Techn.* **18**, 1162 (1970); (*f*) Kolbel, H., and Tillmetz, K. D., *Ber. Bunsenges. Phys. Chem.* **76**, 1156 (1972).
3. Pichler, H., and Burgert, W., *Brennst.-Chem.* **49**, 1 (1968).
4. (*a*) Bhasin, M. M., and O'Connor, G. L., Belgian Patent 824,822 (1975); Wilson, T. P.,

Bartley, W. J., Bhasin, M. M., and Ellgen, P. C., Abstracts, Fifth North American Meeting, Catalysis Society, Pittsburgh, 1977; (*b*) Soufi, F., Thesis, Universität (Th) Karlsruhe, 1969.

5. (*a*) Bond, G. C., "Catalysis by Metals," p. 356. Academic Press, New York, 1962; (*b*) McKee, D. W., *J. Catal.* **8**, 240 (1967).

6. Vannice, M. A., *J. Catal.* **37**, 449, 462 (1975).

7. Fischer, F., Tropsch, H., and Dilthey, P., *Brennst.-Chem.* **6**, 265 (1925).

8. Vannice, M. A., *J. Catal.* **40**, 129 (1975).

9. Schulz, J. F., Karn, F. S., and Anderson, R. B., Bureau of Mines Report of Investigation 6974, 1967.

10. Kertamus, N. J., and Woolbert, G. D., *Prepr., Amer. Chem. Soc. Div. Fuel Chem.* **19**(5), 33 (1974).

11. Eidus, Y. T., Nefedov, B. K., Besprozvannyi, M. A., and Pavlov, Y. V., *Bull. Acad. Sci. USSR Div. Chem. Sci.*, 1129 (1965).

12. Kratel, R., Thesis, Technischen Hochschule, Berlin-Charlottenburg, 1937.

13. (*a*) Natta, G., *in* "Catalysis" (P. H. Emmett, Ed.), Vol. 3. Reinhold, New York, 1955; (*b*) Woodward, H. F., Jr., "Kirk–Othmer Encyclopedia of Chemical Technology," 2nd ed., Vol. 13, p. 370. Wiley, New York, 1967; (*c*) Thomas, C. L., "Catalytic Processes and Proven Catalysts," p. 149. Academic Press, New York, 1970; (*d*) Klier, K., Herman, R. G., and Kobylinski, T. P., Abstracts, Fifth North American Meeting, Catalysis Society, Pittsburgh, 1977.

14. Berty, J. M., *Chem. Eng. Progr.* **70**(5), 78 (1974).

15. Spitz, H. D., *J. Pharm. Sci.* **61**, 1339 (1972).

16. (*a*) Conrad, H., Ertl, G., Koch, J., and Latta, E. E., *Surface Sci.* **43**, 462 (1974); (*b*) Doyen, G., and Ertl, G., *Surface Sci.* **43**, 197 (1974).

17. Kitahara, S., *Bull. Chem. Soc. Japan* **49**, 3389 (1976).

18. Palczewska, W., *Advan. Catal.* **24**, 245 (1975).

19. Maeland, A. J., and Gibb, T. R. P., Jr., *J. Phys. Chem.* **65**, 1270 (1961); Betteridge, W., and Hope, J., *Platinum Metals Rev.* **19**, 50 (1975).

20. Oates, W. A., and Flanagan, T. B., *Canad. J. Chem.* **53**, 694 (1975).

21. Ford, R. R., *Advan. Catal.* **21**, 51 (1970); Eischens, R. P., Francis, S. A., and Pliskin, W. A., *J. Phys. Chem.* **60**, 194 (1956).

22. Hoffmann, F. M., and Bradshaw, A. M., *J. Catal.* **44**, 328 (1976); Bradshaw, A. M., and Hoffman, F., *Surface Sci.* **52**, 449 (1975); Rice, R. W., and Haller, G. L., *J. Catal.* **40**, 249 (1975).

23. Stull, D. R., Westrum, E. F., Jr., and Sinke, G. C., "The Chemical Thermodynamics of Organic Compounds." Wiley, New York, 1969.

24. Hüttig, G. F., and Weissberger, E., *Siebert Festschr.*, 173 (1931).

25. (*a*) Araki, M., and Ponec, V., *J. Catal.* **44**, 439 (1976); van Dijk, W. L., Groenewegen, J. A., and Ponec, V., *J. Catal.* **45**, 277 (1976); (*b*) Jones, A., and McNicol, B. D., *J. Catal.* **47**, 384 (1977); Joyner, R. W., *J. Catal.* **50**, 176 (1977).

26. Wentrcek, P. R., McCarty, J. G., Wood, B. J., and Wise, H., "Abstracts, 172nd National American Chemical Society Meeting," 1976, FUEL006; Wentrcek, P. R., Wood, B. J., and Wise, H., *J. Catal.* **43**, 363 (1976).

27. Rabo, J. A., Risch, A. P., and Poutsma, M. L., Manuscript in press.

28. (*a*) Broden, G., Rhodin, T. N., Brucker, C., Benbow, R., and Hurych, Z., *Surface Sci.* **59**, 593 (1976); (*b*) Joyner, R. W., *Surface Sci.* **63**, 291 (1977).

29. Madden, H. H., and Ertl, G., *Surface Sci.* **35**, 211 (1973); Tracy, J. C., *J. Chem. Phys.* **56**, 2736 (1972).

30. Lloyd, D. R., Quinn, C. M., and Richardson, N. V., *Solid State Commun.* **20**, 409 (1976).

31. (*a*) Bond, G. C., "Catalysis by Metals," p. 76. Academic Press, New York, 1962; (*b*) Sarholz, W., Baresel, D., and Schulz-Ekloff, G., *Surface Sci.* **42**, 574 (1974).

32. Conrad, H., Ertl, G., and Latta, E. E., *J. Catal.* **35**, 363 (1974).

33. Scholten, J. J. F., and Konvalinka, J. A., *J. Catal.* **5**, 1 (1966).